

Migrating subaqueous dunes capture clay floccs

de Lange, Sjoukje I.; van der Wilk, Anne; Chassagne, Claire; Ali, Waqas; Born, Maximilian P.; Brodersen, Kristian; Hoitink, Antonius J.F.; Waldschläger, Kryss

DOI

[10.1038/s43247-024-01901-x](https://doi.org/10.1038/s43247-024-01901-x)

Publication date

2024

Document Version

Final published version

Published in

Communications Earth and Environment

Citation (APA)

de Lange, S. I., van der Wilk, A., Chassagne, C., Ali, W., Born, M. P., Brodersen, K., Hoitink, A. J. F., & Waldschläger, K. (2024). Migrating subaqueous dunes capture clay floccs. *Communications Earth and Environment*, 5(1), Article 729. <https://doi.org/10.1038/s43247-024-01901-x>

Important note

To cite this publication, please use the final published version (if applicable).
Please check the document version above.

Copyright

Other than for strictly personal use, it is not permitted to download, forward or distribute the text or part of it, without the consent of the author(s) and/or copyright holder(s), unless the work is under an open content license such as Creative Commons.

Takedown policy

Please contact us and provide details if you believe this document breaches copyrights.
We will remove access to the work immediately and investigate your claim.

<https://doi.org/10.1038/s43247-024-01901-x>

Migrating subaqueous dunes capture clay flocs

Check for updates

Sjoukje I. de Lange¹✉, Anne van der Wilk¹, Claire Chassagne², Waqas Ali², Maximilian P. Born³, Kristian Brodersen³, Antonius J. F. Hoitink¹ & Kryss Waldschläger¹

Recent research highlights the abundance of floccule (flocs) in rivers, formed by aggregation of clay particles with organic matter. These flocs affect the transport and the eventual fate of clay. Flocs exhibit distinct behaviour from the unflocculated sedimentary counterparts: they can deform and break, and have higher settling velocities, which may in turn cause flocs to deposit and possibly interact with the riverbed. Here, we conducted systematic experiments in a laboratory flume to identify the mechanisms by which flocs and bedforms interact. Flocs showed a saltating (bouncing) behaviour, and were incorporated in the sediment bed as single flocs, clusters, or strings, via deposition and burial in the lee of a dune. Dune geometry was negligibly impacted by the presence of flocs. In natural systems, the burial of flocculated clay particles can affect contaminant spreading, aquatic ecology, the interpretation of deposition patterns, and clay transport.

Flocculated particles (floccule, or flocs), are composed of small mineral particles (so-called primary particles), often clay (<2 µm) or silt (2–63 µm) sized, aggregated to organic matter^{1–7}. They often consist of clay minerals, but also non-clay minerals and grains larger than clay can be found back in flocs. Flocs are not only abundant in estuarine systems worldwide^{8–10}, but prevail in riverine systems as well^{11–14}. Compared to the primary particles that make up the flocs, flocs have lower densities and are several orders of magnitude larger (in the order of 1 mm) than clay particles. This causes settling rates of flocs to be up to 100 times larger, and to have a higher critical shear stress for entrainment¹³. Consequently, unlike primary clay-sized particles, flocs can interact with the sediment-covered bed through settling and entrainment, instead of being transported solely as washload^{13,15}. Understanding the fate of clay, in the form of primary or flocculated particles, is crucial to understand the global carbon cycle¹⁶, to create resilience of coastal landscapes against sea level rise¹⁷, to interpret river-floodplain morphodynamics^{18,19}, to setup sediment budgets²⁰, and to interpret past climates²¹.

The impact of flocculation on clay and total sediment transport rates in rivers has been shown in previous studies^{13,22}. Additionally, it has been acknowledged that clay (potentially in the form of flocs) can be buried in the bed²³. Observed mud deposits in their flume experiments in which they studied the impact of clay on bedforms. They indicate that flow variability (e.g. a very low flow that allows settling of clay) is not needed to produce clay deposits. Furthermore²⁴, conducted flume experiments in which they let the bed aggregate and form bedforms, while continuously

supplying sand and mud to their flume. In the mostly sandy deposits, they also found mud. Despite the observed presence of flocs in the experiments, they could not confirm whether flocs drive the deposition of muddy deposits in riverbeds²⁵. Observed clay aggregates moving as bedload, albeit without interaction with an immobile gravel bed. Similarly²⁶, observed deposition of clay flocs under transport conditions capable of moving sand, despite the low settling velocity of flocs. They also showed how clay can be transported as bed load in the form of floccule ripples²⁷. Indeed, deposited flocs can be found in the Cretaceous (~100 Ma) rock record of mudstone (a clay-rich sedimentary rock)²¹.

Unlike primary particles, flocs can easily deform and break. Deformation alters floc shape, size, and density^{28,29}, while breaking results in the creation of smaller flocs, having the capacity to re-aggregate. In open water, turbulence is the main driver for the aggregation, break-up, and deformation of flocs³⁰. Flocs grow due to increasing collision frequency and thus with higher shear (i.e. flow velocity): mineral clay and organic matter interact to form clay-organic matter aggregates, which are in turn subjected to floc-floc aggregation. Flocs tend to grow larger and less dense under higher organic material contents, both in high salinity³¹ as in fresh water environments³². However, long exposure to shear, or a further increase in shear rate, can lead to a decrease in floc size over time²⁹, as flocs break apart or deform into denser aggregates^{33,34}. These cycles of breakage, regrowth, and restructuring, caused by local hydrodynamic conditions, shape the flocs^{6,28}. If, in the process of settling, the floc is sufficiently strong to withstand the near-bed shear stresses, it deposits on the bed and attaches itself to the bed by cohesive

¹Hydrology and Environmental Hydraulics Group, Department of Environmental Sciences, Wageningen University & Research, Wageningen, The Netherlands.

²Faculty of Civil Engineering and Geosciences, Delft University of Technology, Delft, The Netherlands. ³Institute of Hydraulic Engineering and Water Resources Management, RWTH-Aachen University, Aachen, Germany. ✉e-mail: sjoukje.delange@wur.nl

bonds (either due to its stickiness or due to electrochemical cohesion)^{35,36}. Weaker flocs may break³⁷ and will be re-entrained. Alternatively, individual flocs might not remain intact during the cycles of settling and entrainment, but rapidly reform¹³.

In sand-bedded rivers, near-bed turbulence is primarily influenced by ripples and dunes. Locally, the shear stress increases over a bedform crest and decreases in a bedform trough³⁸. Local shear stress could alter floc size³⁹ and density, and therefore the settling velocity²². The migration of river bedforms mainly determines the bed material load sediment flux, via erosion from the stoss and deposition in the lee^{40,41}. As it has been shown that flocs can deposit on the bed and migrate in as bed load transport in the form of floc ripples^{26,27}, the question arises if and how flocculated particles interact with the migration of river bedforms. Vice versa, bedform geometry, primarily determined by the size of the bed material and the strength of the flow^{42–46}, can be altered by biological processes^{47,48}, pollutants in the water column such as plastics⁴⁹, the size distribution of the bed sediment⁴⁶, and the suspended sediment concentration^{44,50}, yet the impact of flocculated clay on the river bedforms remains unknown. Altogether, the interaction of flocs with bed sediment in a bedform-dominated environment is unclear.

The aim of this study is to enhance our understanding of how flocs are transported, incorporated, and released in bedform-covered systems and to determine whether flocs can influence bedform dynamics. Additionally, we want to explore how flocculation influences the transport of clay particles in bedform-dominated systems. To achieve this, we conducted systematic laboratory experiments in an annular flume, where continuous shear created bedforms in an initially flattened mixed sand-clay bed (2 mass-percentage (m%) of kaolin clay). To simulate riverine environments, fresh water used and an unidirectional flow was imposed. In riverine environments, flocculation is induced by organic material via extracellular polymeric substances (EPS). EPS are natural polymers of high molecular weight secreted by microorganisms, like microalgae. EPS is composed mainly of (exo)polysaccharides. In our experiments, flocculation was induced with a synthetic flocculant. A synthetic flocculant was chosen rather than a bioflocculant, as the former has been well-studied and is well-characterised^{29,33,36,51,52}. Similar to other studies, polyacrylamide-based polymers were used as a proxy for the polysaccharides produced by microorganisms (EPS)^{53,54}, since they have similar flocculation properties (Figure 9 in ref. 55, Figure 6 in refs. 29,32, Section “Preparatory experiments to define the parameter space”). During the experiments, two shear stress values and six flocculant dosages were imposed, resulting in diverse bedform sizes and different degrees of clay flocculation. Dune and floc characteristics were measured and visual imaging provided insights into floc-sediment bed interactions.

Results and discussion

Response of flocs to turbulent shear

After three hours of experimental run time, we sampled flocs at 10 cm above the mean bed level (about half the water depth), and subsequently measured their sizes using a settling column with a camera setup (Section “Instrumentation”). The measured floc size seemed to be influenced by shear stress. Under lower shear stress (0.35 N m^{-2}), flocs tended to be larger, with an average size of $75 \mu\text{m}$ (averaged based on floc count), compared to $59 \mu\text{m}$ in higher shear conditions (0.5 N m^{-2}) (Fig. 1). The variation in floc size was also greater in low shear conditions, with a standard deviation of $55 \mu\text{m}$, compared to $37 \mu\text{m}$ in high shear. This suggests that turbulence plays a role in breaking up flocs into smaller, more compact particles that are less likely to disintegrate, as supported by previous research²⁸. We found that beyond a certain flocculant concentration (0.46 mg g^{-1}), the increase in floc size levelled off. Combining this with the observed reduction in variability at higher shear supports the idea that floc size is constrained by turbulence, rather than the potential to flocculate⁵⁶.

The smallest eddies in turbulent flow, defined by the Kolmogorov length scale η ^{57,58}, are often seen as the upper limit for floc size. In our study, η was estimated using flow conditions (see Eq. (2) in the Method section)¹⁵. At 10 cm above the mean bed level, η was $332 \mu\text{m}$ for low shear and $291 \mu\text{m}$ for

high shear, which are much larger than the largest measured flocs ($183 \mu\text{m}$ and $129 \mu\text{m}$ at the 95th percentile, respectively).

However, local shear stress –and thus η – varies depending on the position relative to bedforms. In our experiments, the bedforms averaged between 0.030 and 0.093 m in height and 0.63 to 1.3 m in length, for low and high shear conditions, respectively. As acknowledged in literature, flow velocities were highest above the dune crests, while the conditions were calmer in the dune troughs^{38,59}. The high shear over dune crests seems to set an upper limit for floc size, and η decreases when approaching the bed. For instance, at a depth of roughly 2 mm (equal to a relative depth, i.e. depth divided by total depth at that point, of 0.01) above the dune crest during high shear, η was $86 \mu\text{m}$, while it was $103 \mu\text{m}$ in low shear conditions. Similarly, in the dune troughs (at around 3 mm above the bed, at a relative depth of 0.01), η was estimated to be $97 \mu\text{m}$ during high shear and $107 \mu\text{m}$ in low shear. This shows that larger flocs can exist in low-shear areas and in dune troughs before they break apart or deform. Since η generally decreases with decreasing distance from the bed, flocs that interact with the bed experience smaller turbulent whirls closer to the bed than higher in the water column. Lower shear stress might therefore also lead to a more stratified distribution of the flocs in the water column (due to a smaller gradient of η), which would impact the sampled floc sizes.

Overall, the near-bed shear stress seems to act as a good first indicator of floc size. However, the actual flow above bedforms is complex and not uniform (as are the shear stresses flocs encounter in the natural environment²⁹), which means our estimations are based on simplified conditions. In field conditions, the shear stress above dune crests is higher than the depth-averaged stress³⁸, which could explain why average floc sizes are smaller than the values predicted by η . The dynamic nature of shear stress could mean that flocs do not always reach equilibrium within the flow, although the similarity between floc sizes and η suggests they may still be influenced by it. In cases where the dunes have a steep leeside angle, flow separation occurs on the leeside^{60,61}, creating a recirculation zone that can trap flocs. This could lead to flocs breaking apart over dune crests, while allowing them to settle and aggregate in the more sheltered dune troughs.

Clay transport in the presence of flocs

Shortly after the start of the experiments, bedforms began to develop, resulting in the washing out of the clay (i.e. winnowing⁶²) from the active bed (i.e. all sediment that is in motion, or recently has been in motion) due to bedform migration (Fig. 2a, b). This process, referred to by ref. 63 as ‘deep cleaning’, has been observed for primary clay particles in sand-clay mixtures with a clay content of less than 8 – 12.6% in the past, and leads to suspended transport of the clay particles^{62,63}.

With the presence of a flocculant, suspended clay particles can aggregate and form flocs, even in experiments with very low flocculant concentration. The ~ 100 -times larger size of the flocs increases their settling velocity to about 1 mm s^{-1} (measured in the settling column), allowing interaction with the sediment bed. In our experiments, the flocs are transported as mixed-load: they are partially transported in suspension, while also saltating over the bed (Fig. 2b). Saltation refers to the bouncing motion of particles, where they are being lifted up and transported, before depositing. Flocs can saltate over the stoss side of the dune without breaking up (Fig. 2b-1–5). Especially larger flocs, which have a higher settling velocity, interact more with the bed. At the crest of the dune, where the shear is the largest, the flocs can break and resuspend (Supplementary Fig. S3), or saltate down the leeside of the dune (Fig. 2b-6). The flocs can be trapped in the leeside, by the recirculating current caused by flow separation.

Clay incorporation in the bed

Dunes migrate by erosion of sediment particles from the stoss side and deposition at the leeside^{40,41}. We observed flocs being trapped in the leeside of the dunes. There, they may attach to the bed through cohesive bonds³⁶, increasing their resistance to erosion. Flocs that have deposited in the recirculation zone of the leeside are subsequently incorporated or buried in the bed by the migration of dunes.

The incorporation of flocs within the dune (Fig. 3) can occur at the scale of an individual floc, a cluster of flocs, or a floc string. An individual floc may stagnate on the leeside of the dune (Fig. 3a–1, a–2), where the recirculating flow and the current balance each other out. Subsequently, denser grains avalanche down the leeside and bury the stagnant floc (Fig. 3a–3). Depending on timing and quantity of sand avalanching, a different amount of flocs accumulated in the lee. Over time, a cluster of flocs may form on the leeside of the dune, which subsequently gets buried. This happens when a turbulent pulse mobilises a large amount of sand grains, causing them to avalanche over the floc deposit (Fig. 3b). With even more time, a string of flocs can cover almost the entire leeside of the dune (Fig. 2c), with new flocs adhering to formerly deposited flocs, creating a multi-layered deposit, offering shelter from erosion. The classical erosion-deposition pattern within a dune exhibits diagonally-oriented string-like structures at an angle similar to the leeside angle of the dune (Fig. 2c). These laminae (i.e. foresets⁶⁴) have also been observed in the burial of non-deformable objects such as plastics⁴⁹ and charcoal⁶⁵.

Generally, a higher concentration of flocs resulting from an increased flocculant amount led to more flocs being temporarily buried in the dunes. At higher shear stresses, smaller flocs were observed than at low shear stresses (Section “Response of flocs to turbulent shear”); however, the higher mobility of the dunes resulted in more visible burial of flocs in the dune. Similarly⁶⁵, suggested that the amount of charcoal deposition is related to bedform migration rates. It is yet unclear how different floc sizes alter the interaction between flocs and the sediment bed, which may be subject to further study.

Altogether, this means that while primary clay particles are washed out from the bed when entrained, they can be incorporated into the bed through the migration of dunes, which bury the trapped flocs in the form of organised multilayered floc-clusters (group deposits).

The influence of flocs on dune geometry

Under continuous shear, the sediment bed developed into bedforms (Supplementary Figs. S4), often featuring dunes with superimposed ripples. The ripples had a relatively constant near-equilibrium height, length and leeside angle at both imposed shear stresses ($\Delta_r = 0.016$ m, $\lambda_r = 0.24$ m, $LSA_r = 9.8^\circ$). This behaviour was expected, since ripple geometry is related to particle size of the bed material, and is independent of flow velocity^{43,66–68}. As expected, near-equilibrium dune geometry shows a clear relation with shear stress^{42,43,69–72}. Dunes in the higher shear stress regime are three times as high and twice as long ($\Delta_d = 0.093$ m, $\lambda_d = 1.3$ m) compared to dunes in the lower shear stress regime ($\Delta_d = 0.030$ m, $\lambda_d = 0.63$ m), although leeside angle remains constant ($LSA_d = 9.5^\circ$). Dune height of all dunes at the end of each experiment was relatively well-predicted with the dune height predictor of ref. 42 (0.083 m), independent of clay and flocculant concentration.

Near-equilibrium bedform geometry is not directly affected by flocculant amount or floc size (Table 1, Supplementary Fig. S5). This opposes the findings in ref. 47. They mixed flocculant (in their case, Xanthan gum as a proxy for EPS) into the sediment bed, which resulted in a significant decrease in dune height. In their experiments, EPS resulted in clay and sand grains sticking together, while in our experiments, the clay only flocculated with itself. This can explain why the dune height in our experiments is only

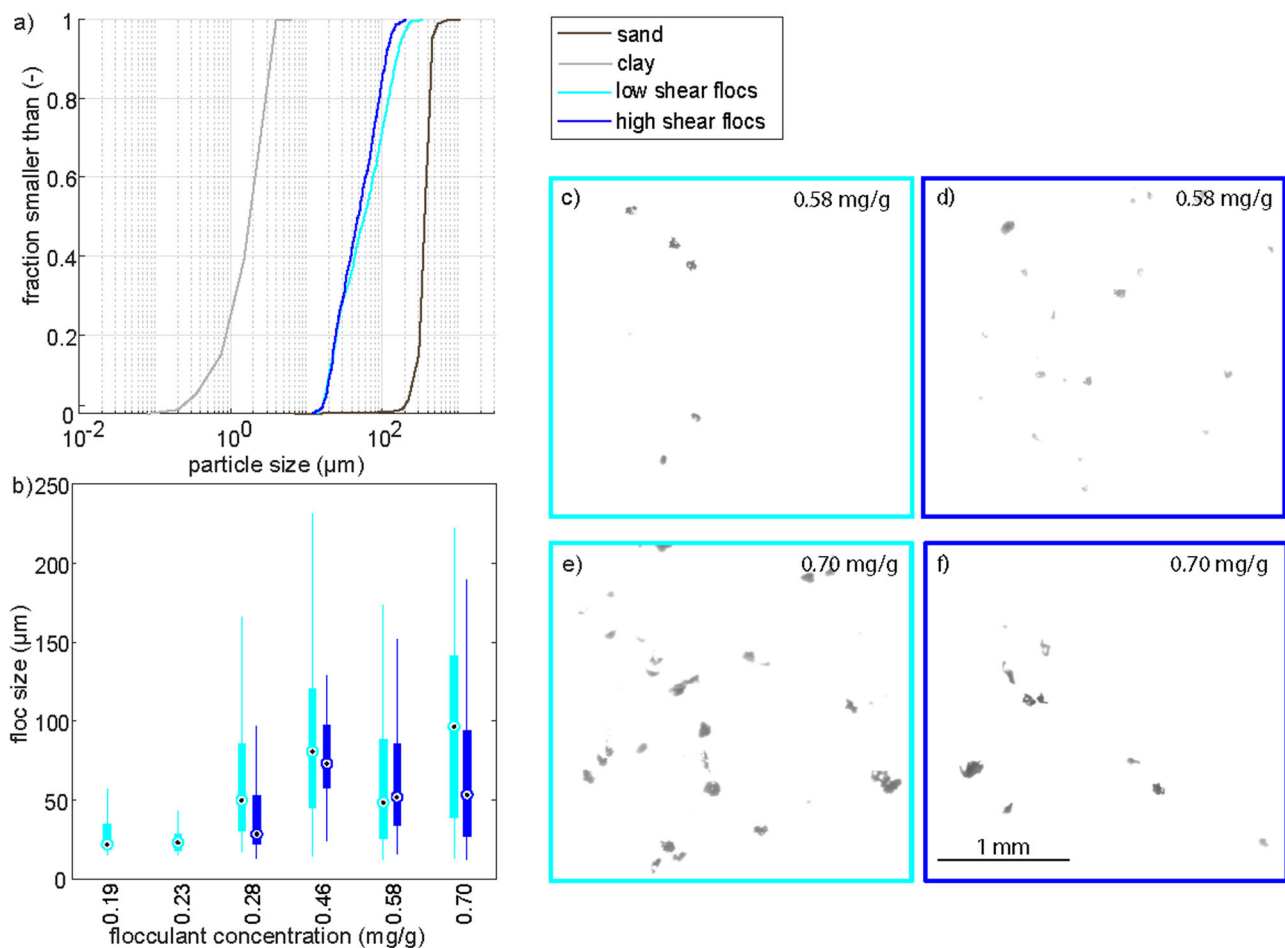


Fig. 1 | Floc characteristics subject to study. **a** Cumulative size distribution of sand and clay used in the experiments, and flocs from high and low shear experiments combined. **b** Floc size during the experiments. The central box represents the interquartile range (Q1–Q3), with the black dot indicating the median. Whiskers

extend to the smallest and largest data points within 1.5 times the interquartile range from Q1 to Q3. Outliers are not shown. **c–f** Example pictures of the flocs as taken by the floc camera. Flocculant concentrations are noted in upper right corner.

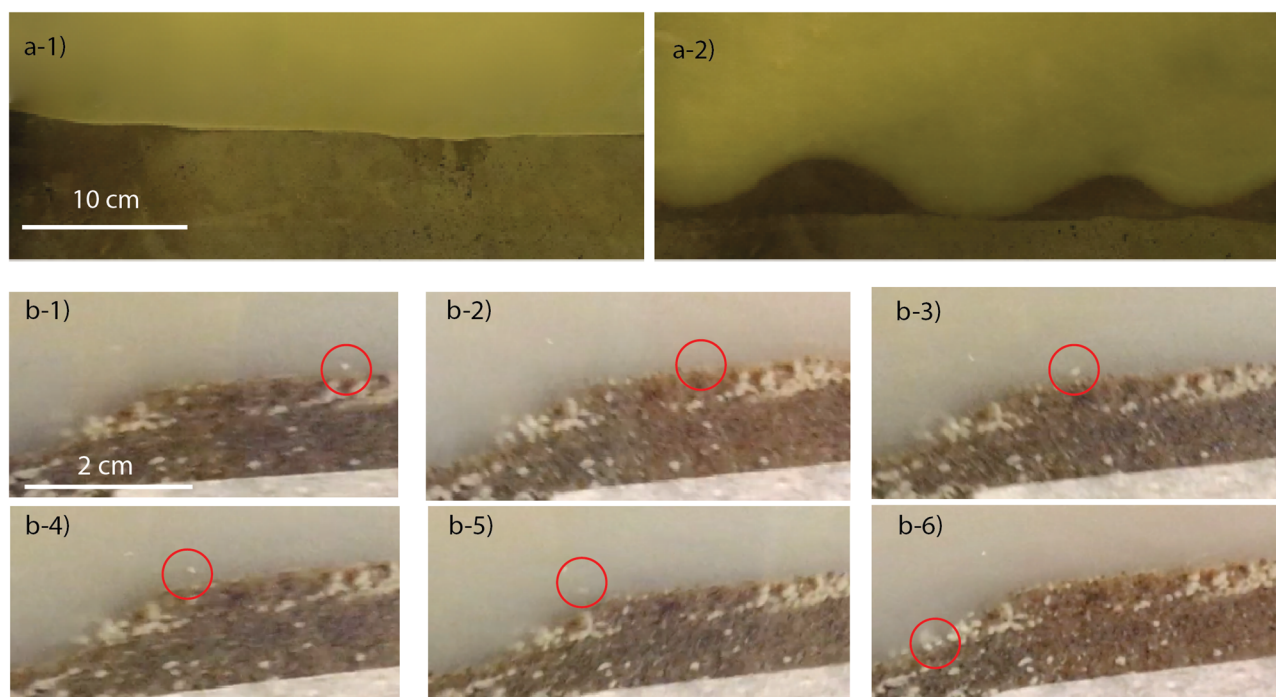


Fig. 2 | Transport of clay. **a** Homogeneously mixed primary particles of clay (**a-1**) are washed out from the active bed into the water column (**a-2**). The image is slightly adjusted to remove reflections. **b** Saltating behaviour of an individual floc (**b-1–4**), which is almost re-entrained into the water column (**b-5**), but ultimately becomes

trapped in the leeside of the dune (**b-6**). Images taken with a mobile phone with a frame rate of 30 fps. Flocs can easily be detected by their white colour compared to the brown sand. Flow direction from right to left.

slightly affected. The difference in flocculation behaviour can potentially be explained by the amount of flocculant added. Although the two flocculants are not directly comparable, our flocculant percentage was lower (maximal 0.7 mg/g of clay, i.e. 0.001 m% of all sediment) than their flocculant amount (maximum 0.1 m% of all sediment). Additionally, the difference in mixing method (i.e. mixing the flocculant into the bed or injecting it in the water) might play a role⁷³, however, we found that under our experimental settings, floc characteristics were independent of the mixing method (Section “Preparatory experiments to define the parameter space” and Supplementary Materials S1).

Despite the lack of clear trends in dune geometry development, we did observe a slight, non-significant, increase in dune height and length with increasing flocculant amount under low shear conditions ($R^2 = 0.62$ and 0.71 , respectively). Contrarily, the incorporation of plastic particles (1–10 mm) in dunes as researched by ref. 49 did lead to altering of dune geometry. Pits or scours formed when plastic particles migrated towards the dune crest from the stoss side. Alternatively, they observed “bursts” of a cluster of plastic and sediment, being eroded rapidly from the stoss side, resulting in shorter dunes with steeper stoss sides. The cohesive character of the flocs in our experiments might have prevented this.

In our experiments, a potential lengthening of the dunes with floc size appeared insignificant ($p > 0.05$; Table 1). Erosion of flocculated particles from the stoss side (Fig. 3a, c) did not create a pit as observed by ref. 49, nor were there observed bursts of flocs. The former could be explained by flocs being generally smaller than the sediment grains, while the plastic particles were larger than the grains. Hence, erosion of an individual floc from the stoss insignificantly impacted the stoss side. The fact that no mass erosion of flocs occurred, contrary to the bursts of plastics, might relate to the organic nature of the flocs. According to ref. 36, upon settling, flocs form cohesive bonds with the bed and with each other, resulting in a higher erosion threshold than expected based on their density, potentially preventing simultaneous entrainment of entire floc strings. Although flocs stick easily to other flocs, the strength of floc-sand cohesion is unknown. Regardless of

this, similar to a small percentage of primary clay particles in the bed⁶³, cohesion seems to be insufficient to limit bedform growth as in refs. 45,47,73. Instead, a slight increase in dune length with flocculant concentration is observed for low shear stresses. At higher flocculant concentrations, more flocs are buried in the bed. The effect on dune length can be related to their lower erosion threshold (e.g. critical shear stress) compared to sand particles of the same size due to their lower densities, likely increasing their transport stage (ratio of shear stress and critical shear stress). A higher transport stage generally results in longer dunes⁴². This effect could be larger for larger, less dense flocs, and vice-versa for smaller, denser flocs, but confirmation of this hypothesis should come from tailored experiments.

Conclusion and implications

The photo in Fig. 4a visualises the key aspects of floc interaction with the bed. Clay in the water column is transported as suspended load, as primary or as flocculated particles (Fig. 4a-I). These flocculated particles settle rapidly if the flow is halted (Fig. 4a-II), which may represent low river flow conditions or slack tide in nature. During active sediment transport, the larger flocs are transported via saltation (Fig. 2b). This leads to clay being captured in dunes in the form of flocs (Fig. 4a-III), either individually, as clusters of flocs, or as floc strings. Flocs that are trapped in the leeside recirculation zone can be buried by grains avalanching down during a turbulent pulse. Continuous erosion and deposition processes of bedforms of various heights can result in the emplacement of floc drapes just below the currently active bed, as a result of previous migration of larger bedforms (Fig. 4a-IV). Below the active bed, the clay particles remain mixed within the sand bed (Fig. 4a-V).

The interaction of clay with the bed is summarised in Fig. 4b. Floc deposition is concentrated in areas with low shear and a higher Kolmogorov length scale (dune trough). Floc transport occurs over the dune stoss, where shear stresses are larger and the Kolmogorov length scale is smaller. The variability in shear stress due to the geometrical complexity of the bed allows for the trapping of flocs. Despite their deformability, flocs behave similar to

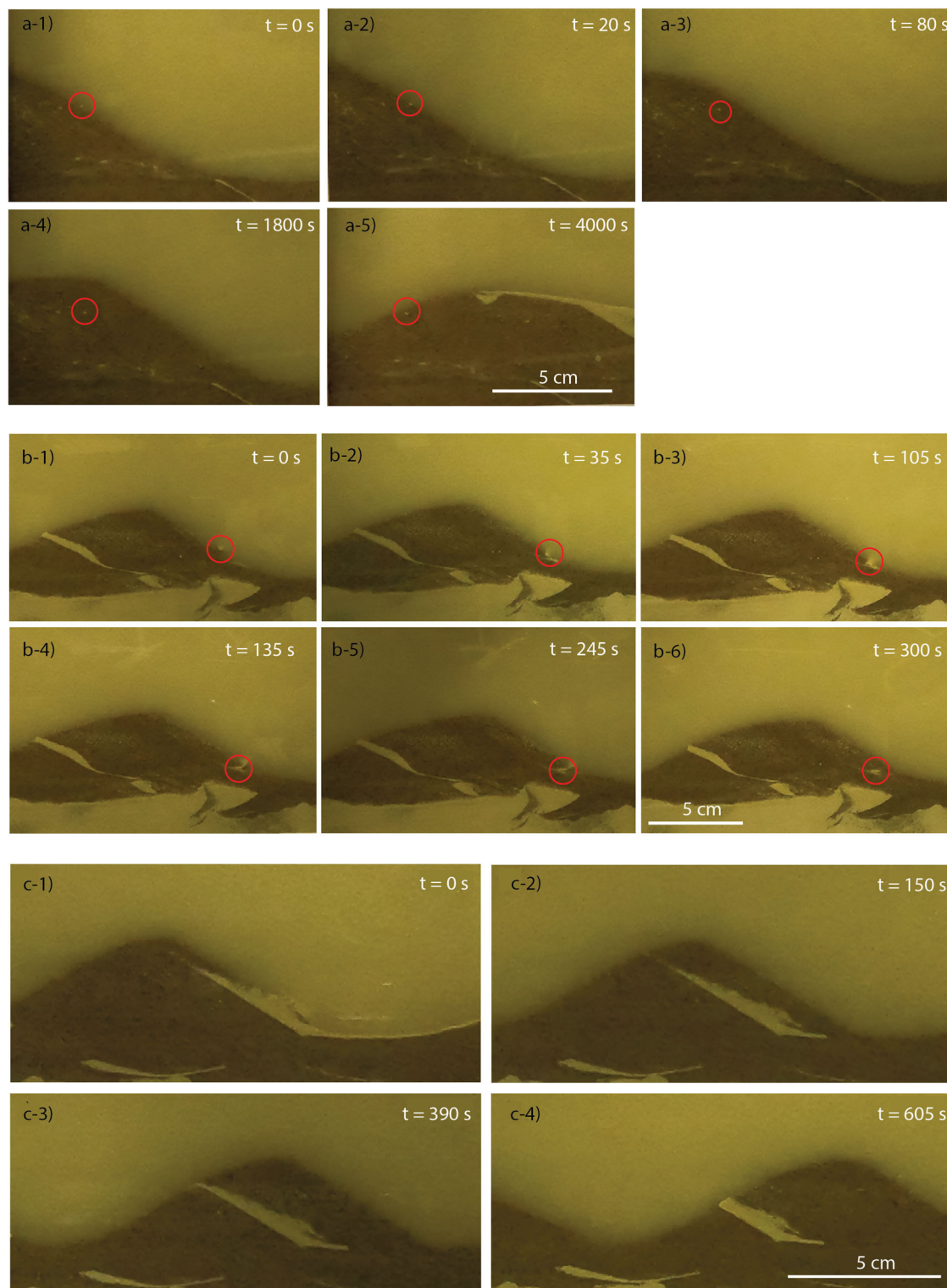


Fig. 3 | Transport of flocs and burial in the sediment bed. Images are taken every 5 s with a GoPro 6 camera, allowing to track settled flocs. Flow direction from left to right. **a** Burial of an individual floc into a dune (experiment 10). **b** Burial of a cluster of flocs (experiment 13). **c** Burial of a string of flocs in the bed (c-1, c-2) and the subsequent re-entrainment into the water column (c-3, c-4) (experiment 13).

plastic particles⁴⁹ and charcoal¹⁶⁵. At the top of the dune, where shear stresses are greatest, the fate of flocs is determined as flocs are either resuspended or trapped in the lee.

Although other researchers have shown that fine sediment flocs are incorporated into riverine sandy beds (e.g. refs. 23,27 and 24), to the best of our knowledge, this present study is the first to demonstrate the mechanisms

through which this process occurs. This incorporation of flocs into the sediment bed has important impacts across a range of disciplines.

Regarding environmental toxicology, the burial of flocs must be considered in contaminant studies. Flocs are key elements of contaminant transport, such as organic pesticides and heavy metals, due to the adsorption of the contaminant to the floc^{20,74}. Our study shows that the residence time of

Table 1 | The strength of the relation between dune geometry and floc characteristics, expressed in R^2

R^2	Dune height (m)		Dune length (m)	
	Low shear	High shear	Low shear	High shear
Flocculant concentration (mg g^{-1})	0.62*	0.03	0.71*	0.29
Floc size (μm)	0.09	0.23	0.22	0.24

The strength of the relation is expressed in R^2 .

*Indicates a significance level of $0.05 < p < 0.1$. None of the relations has a significance level of $p < 0.05$. Supplementary materials S5 shows the corresponding scatter plots.

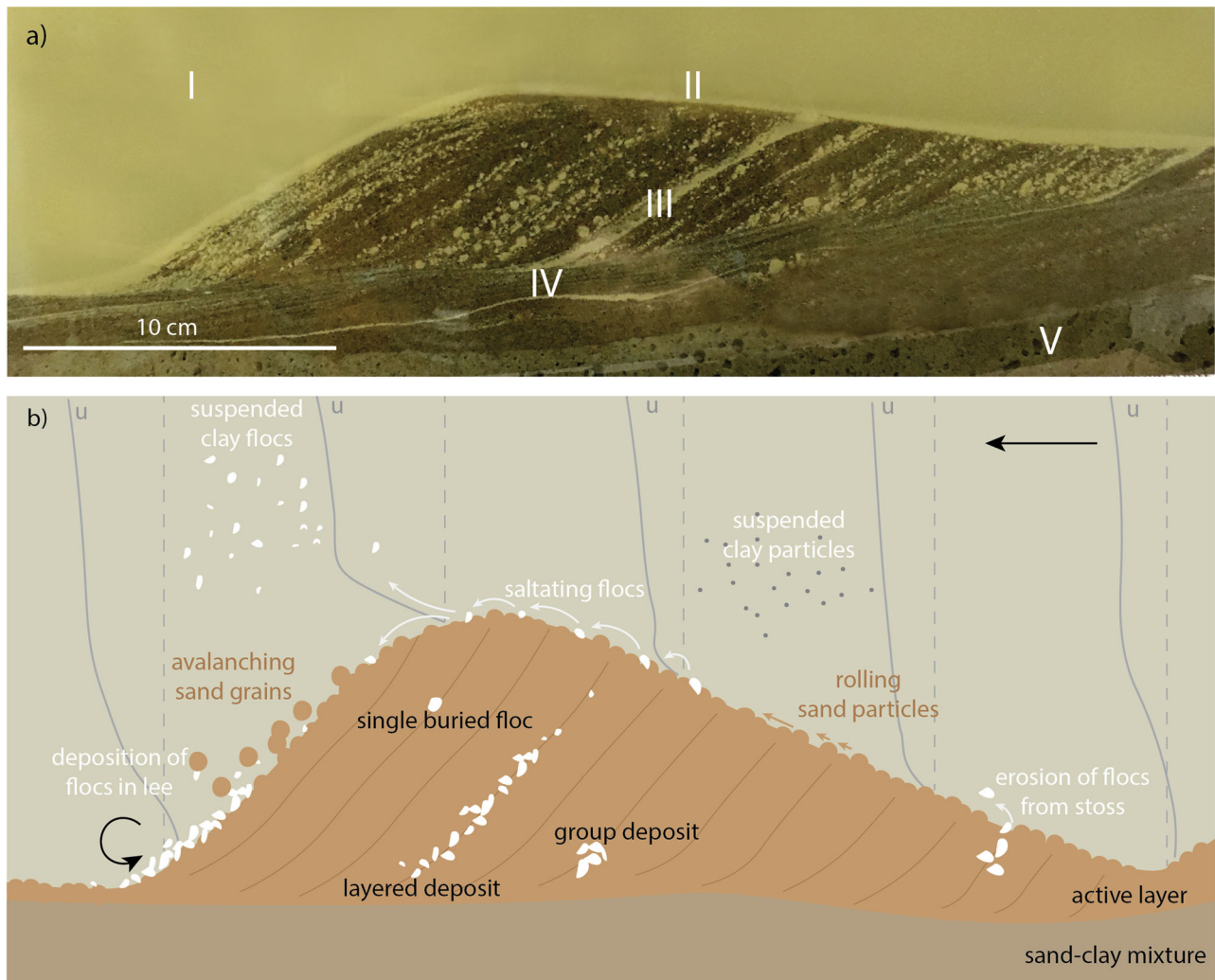


Fig. 4 | The possible fate of clay in rivers. a Capturing of flocs in a bedform, in which five regimes are indicated, I: suspension, II: recent deposition, III: drapes within a dune, IV: drapes below the active surface (remnant), V: homogeneously mixed conditions (initial experiment conditions). The image is taken seconds after the flow has halted. In this time a depositions layer of flocs has formed on the dunes. The

image is slightly adjusted to reduce reflections. **b** Schematic of the suspended and bed load transport of clay particles and flocs, and the subsequent trapping in the sediment bed. Velocity profiles (u indicates the flow velocity, dotted line indicates zero m s^{-1}) are schematised based on the measurements in ref. 38.

these clay-bound contaminants might be altered, by being easily incorporated in the bed sediment via flocs. These may then be re-entrained during higher discharge events^{75,76} that feature larger dunes, with a deeper active bed. Additionally, microplastics could be entangled in flocs or could behave as flocculant^{77–79}. With the expected rise in plastic waste in the future⁸⁰, the incorporation of microplastics in the bed via the process of floc burial might become a severe problem.

Sedimentologically, clay in deposits can serve as a proxy for fine sediment supply²⁴ and ancient flow conditions³⁶. As shown by ref. 23, our experiments confirm that clay occurrence in deposits (e.g. mud drapes) does

not only indicate past flow conditions which are variable⁸¹, such as during slack water in a tidal cycle⁸² or calm^{83,84}, but also could indicate steady shear. This suggests that conclusions drawn from sediment deposits containing clay may need to be reconsidered²⁶. This is confirmed by ref. 21, who tracked composite particles (flocs) in sedimentary rocks, and acknowledged that mudstones consist of much coarser-grained components (flocs) than suggested by their petrographic composition (clay). The burial of mud in the bed is substantial²⁴, and we now showed that this can relate to flocculation, even in riverine systems that were, until recently, considered to have minimal floc formation.

Regarding sediment transport, floc capturing in the bed needs to be considered for mud transport modelling in various contexts^{85,86}. The smallest aggregate persisting in a particular flow field may easily contain hundreds of clay particles^{87,88}, and the burial of these flocs can alter clay transport rates. The in situ study carried out by ref. 89 showed that fluid mud, consisting of flocs, were deposited during slack water conditions, and were entrained once the flow regained strength. Our study indicates that floc deposition can also occur during higher flow conditions due to the migration of dunes. The expected mud content in recently deposited clay is relevant for the compaction rate and subsequent subsidence, and the stability of river banks⁹⁰. The significance of the burial of flocs in the bed for clay transport needs to be studied further, with a potential adjustment of numerical clay transport models as a result.

Ecologically, studies of riverine systems must consider the increased burial of clay flocs into the bed. Flocculation of clay removes clay from the water column, which alters the light climate^{91,92}. Additional burial of flocs within the bed could amplify this effect. Furthermore, an increased concentration of clay lenses in the bed could reduce hyporheic exchange, which may be problematic for biota living in the sediment that rely on gas exchange⁹³.

In essence, this study suggests the need for a more critical look on the transport mechanisms of flocs and clay. It is essential to further investigate how flocs become buried in the sediment bed of rivers, and to quantify the effect of floc capturing, both in the lab and in the field.

Methods

Preparatory experiments to define the parameter space

A series of preliminary settling and rotating wheel experiments were carried out in the joint Deltares-TU Delft laboratory in Delft, the Netherlands. With these tests, the materials for the main experiments (i.e. suitable flocculant type and dosage, clay type and concentration) as well as the mixing method for the flocculant were determined. Additionally, the response of the flocs to shear was assessed. The tests are described in Supplementary Materials Text S1 and their results are summarised below.

Natural "flocculant", EPS, as found in nature by excretion of microorganisms, is composed mainly of (exo)polysaccharides. It can include other molecules such as DNA, lipids and humic substances, for example, the EPS used by ref. 32 contains 2.64% of proteins for 97.35% of polysaccharides. Despite the fact that the chemical composition and structure of different EPSs are different, all EPSs display the same flocculation properties. The differences in composition and structure results in changes in flocculation kinetics and maximum size of flocs obtained. However, the growth in particle size of flocs follow the same trends: upon addition of flocculant, the aggregation between sediment and flocculant is initiated and flocs grow fast in a few minutes to their maximum size. After reaching their maximum size, the average size of flocs is decreasing slowly over time as flocs reconform under shear. Polyacrylamide (PAM) flocculants as used in this study, are commonly used in wastewater treatment and therefore widely studied^{33,51,52,94}. They are hydrophilic polyolefins (polyethylenes with amide substituents on alternating carbons) and commonly used as flocculating agents in water treatment plants. The flocculation mechanism of PAM is very similar to the one of EPSs^{29,32,55}.

PAM flocculants are either cationic (positively charged) or anionic (negatively charged). In this study, a cationic flocculant ZETAG - 8125⁹⁵ was selected, which is a copolymer of acrylamide and quaternised cationic monomer, of low cationic charge and high molecular weight. Using a cationic polyelectrolyte, in contrast to the use of an anionic polyelectrolytes, the polymer-clay flocculation is mainly driven by the electric interaction between the positively charged polymer and the negatively charged clay particles, irrespective of salinity. This prevented cumbersome water quality analysis and matching water properties, as tap water was used.

Flocculant dosage impacts floc size and their resistance (strength) to shear^{29,51}. Its optimal dosage for the experiments was determined based on the preparatory tests. The test parameters were based on a lower limit

Table 2 | Experiments (number #) and their corresponding test parameters

#	Shear stress (N m ⁻²)	Clay (m%)	Flocculant*		
			g	mg L ⁻¹	mg g ⁻¹
1, 2	0.35, 0.5	0	0	0	0
3, 4	0.35, 0.5	2	0	0	0
5	0.35	2	1.5	5.9	0.18
6	0.35	2	1.9	7.4	0.23
7, 8	0.35, 0.5	2	2.3	9.0	0.28
9, 10	0.35, 0.5	2	3.7	15	0.46
11, 12	0.35, 0.5	2	4.7	18	0.58
13, 14	0.35, 0.5	2	5.7	22	0.70

*The amount of flocculant in the experiments is shown in grams, milligram per litre of water, and milligram per gram of clay.

inferred from the detection limit for the floc camera, being 20 µm, and an upper limit determined by the optimum flocculant concentration. An increasing amount of flocculant leads to the formation of flocs containing a large amount of flocculant, which have slower flocculation kinetics than flocs formed at smaller dosages. Well above the optimum flocculant concentration, unflocculated polyelectrolytes remain in suspension^{29,51}. In our experiments, we remain below the optimum concentration to prevent an increase in water viscosity caused by an overdose of flocculant^{51,96}. Kaolin clay with a D_{50} of 1.3 µm was used as primary mineral clay particles. The clay concentration was decided to be 2 mass-percentage (m%) (relative to the sand; 0.5-volume% relative to the water). This was sufficient to form substantial flocs, without the clay substantially impacting flow dynamics⁹⁷ or impeding bedform growth (as seen in refs. 50,63,98).

The appropriate shear stress was determined to fall within the dune regime⁹⁹, while preserving floc integrity¹⁰⁰ (Table 2). This was tested in preliminary experiments, where we observed that flocs interacted with the bed by being buried and re-entrained. As anticipated, flocs were smaller when exposed to shear^{29,34}, yet the determined dosages remained accurate. Finally, the mixing method was tested, from which it was found that the final floc characteristics are insensitive to the mixing method.

Experimental setup

The experiments took place in an annular flume in the hydraulic lab of the Institute of Hydraulic Engineering and Water Resources Management (IWW) at RWTH Aachen University, Germany. The flume, with a diameter of 350 cm, a width of 25 cm, and a height of 100 cm (Fig. 5), was preferred over other types of flumes for its ability to recirculate water without necessitating pumps, which could break or deform the flocs^{101,102}. Water flow was generated through rotation of a lid, while the counter-rotation of the flume limited secondary currents^{103,104}. The ratio between lid and flume rotation was chosen such that the centrifugal forces balance each other¹⁰⁵, converting the annular flume into a representation of an infinite straight river.

The flume was filled with a 10 cm layer of mixed sediment, consisting of medium sand with a median grain size (D_{50}) of 350 µm, and 2 m% kaolin clay with a D_{50} of 1.3 µm. Before each experiment, the sediment bed was levelled, and the flume was filled with 20 cm tap water. The cationic flocculant was dissolved and mixed overnight before each experiment, to ensure a complete solution and a uniform distribution in the flume. Just before the experiment, the flocculant was added to the water in the flume.

Each experiment ran for 4 h, with a total duration of 5.5 h to accommodate bed level measurements (Section "Instrumentation"). The second bed-level survey was taken 45 min after the first, after which the measurement frequency was increased to every 30 min for the last four surveys. Throughout the experiments, the water temperature was 22.6 °C (standard deviation $\sigma = 0.8$), with an electrical conductivity of 310 µS m⁻¹ ($\sigma = 22$) and

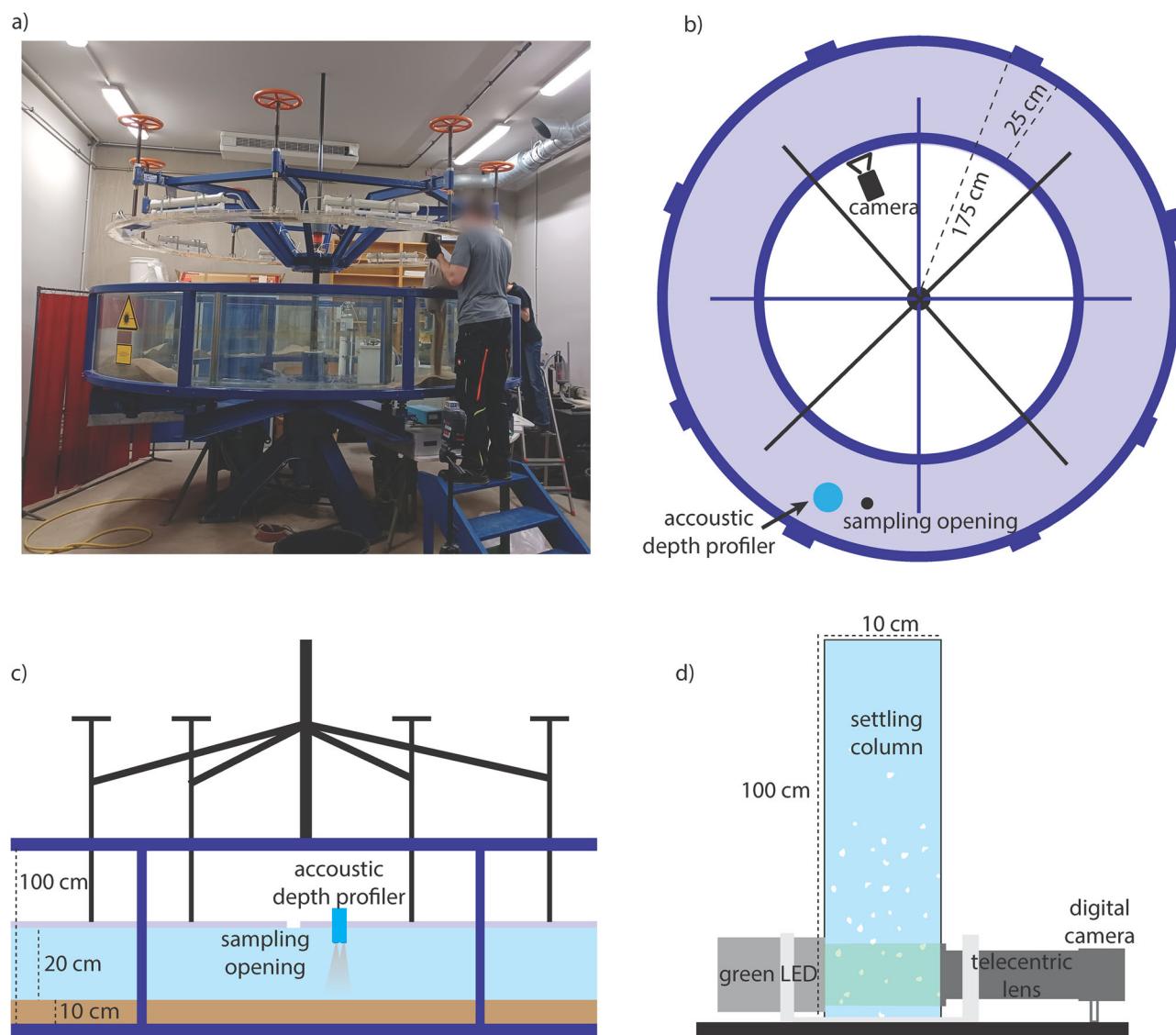


Fig. 5 | Experimental setup. A picture (a), schematised top-view (b) and schematised side view (c) of the annular flume. **d** Side-view of the settling column setup. Subfigure (b–d) are not to scale for visualisation purposes.

a pH of 7.4 ($\sigma = 0.4$). After each experiment, the bed was levelled, and the shear stress and flocculant amount were adjusted to match the next experimental setting.

The parameter set tested was determined through the preparatory experiments (Section “Preparatory experiments to define the parameter space”), and is described in Table 2. Six different flocculant amounts were used in the experiments, ranging from 0 to 22 mg L^{-1} (corresponding to 0.7 mg g^{-1} clay and 13 mg kg^{-1} total sediment). Four base experiments were conducted for the two different shear stresses, including two with no clay and no flocculant, and two with only sand and clay, but no flocculant. This enabled us to observe deviations from conditions without flocs present. Two different shear stresses, 0.35 and 0.5 N m^{-2} , were tested, such that all experiments fall within the dune regime⁹⁹, while preserving floc integrity¹⁰⁰. Imposed shear stress was determined based on the ratio between the lid and flume rotation¹⁰⁵. For the two lowest flocculant dosages, only the low shear stress conditions were tested, as flocs were very small during these experiments, and would not have been visible under higher shear conditions.

Instrumentation

An acoustic depth profiler, the StreamPro Acoustic Doppler Current Profiler (hereafter StreamPro), manufactured by Teledyne, was used to measure

bed elevation, from which bedform geometry was derived (Section “Data analysis”). This acoustic device is capable of penetrating turbid water. The StreamPro was attached to the moving lid of the flume, positioned 7 cm from the outer edge. By rotating the flume, four profiles corresponding to the four beams of the StreamPro could be measured, with a frequency of 1 Hz. To ensure a millimetre resolution, the rotational speed of the flume bottom was temporarily reduced to 0.11 rotations per minute for the measurements, after which the rotational speed was increased again to the experimental shear stress. Any temporarily deposited flocs were directly resuspended by the accelerating flow.

A $10 \times 10 \times 100 \text{ cm}$ settling column was used to determine floc characteristics (Fig. 5d), following a setup similar to refs. 106 and 54. After three hours of experimental run time, flocs were collected from 10 cm below the water surface and at the top of the sediment bed. A 25 mL pipette was used to carefully extract flocs from the flume, and by subsequently touching the water surface of the settling column the flocs could flow into the settling column with minor disturbance. The characteristics of the captured flocs were recorded using a UI-3160CP Rev. 2.1 floc camera from IDS with a TC23024 lens from Opto Engineering. A green light (LTCLHP024-G from Opto Engineering) was used to illuminate the flocs in the settling column. The floc camera was controlled using the uEye cockpit software developed

by IDS, configured to produce monochrome images for improved contrast to visualise the flocs.

A GoPro 6 was positioned in the middle of the flume, facing outward, to record bed evolution during the experiment at a fixed location, covering ~45 cm in width, and the whole water depth. Pictures were taken every 5 s.

Data analysis

For the analysis of the flocs, the images from the floc camera were processed using the SAFAS software (Sedimentation and Floc Analysis Software)¹⁰⁷. Subsequently, the settling speed of the flocs, and the major and minor axis diameters of the flocs were determined. Throughout the experimental runs, there is a balance between breakage and aggregation of flocs, leading to the attainment of equilibrium in floc size²⁸. The floc diameter D_f was then computed as¹⁰⁶:

$$D_f = \sqrt{D_{major} * D_{minor}} \quad (1)$$

The Kolmogorov length scale, η (m), is known to correlate with the size of the flocs and can be approximated with¹⁵:

$$\eta = \left(\frac{\kappa z \nu^3}{u^*{}^3 \left(1 - \frac{z}{h}\right)} \right)^{\frac{1}{4}} \quad (2)$$

in which κ is the Von Karman constant, ν the kinematic viscosity of water ($\text{m}^2 \text{s}^{-1}$), u^* the shear velocity (m s^{-1}), z the height above the bed (m) and h the water level (m).

The shear velocity u^* was calculated by using the bed shear stress τ (N m^{-2}) and the density of the water ρ_w (kg m^{-3}), via:

$$u^* = \sqrt{\frac{\tau}{\rho_w}} \quad (3)$$

For the analysis of the bed level, the StreamPro data was processed using ADCPTOOLS¹⁰⁸, and bed elevation profiles from each of the four beams were determined. These profiles served as input for the bedform tracking tool from¹⁰⁹, which gives bedform geometry based on specific span values used to differentiate between different bedform scales. Two bedform lengths were identified: $0.2 \text{ m} \pm 0.1 \text{ m}$ (hereafter referred to as ripples) and $2.2 \text{ m} \pm 0.8 \text{ m}$ (referred to as dunes). In almost all experiments, ripples were superimposed on dunes.

Bedform characteristics were averaged over the four beams. The characteristics include: (1) bedform height Δ (m), the vertical distance between top and downstream trough, (2) bedform length, λ (m), the horizontal distance between two subsequent crests, (3) leeside angle, LSA ($^\circ$), the slope from a linear fit of the bedform's leeside, excluding the upper and lower 1/6 of the bedform height and (4) the stoss side angle and SSA ($^\circ$), calculated similarly to the leeside angle.

Reporting summary

Further information on research design is available in the Nature Portfolio Reporting Summary linked to this article.

Data availability

Data used in this study can be accessed via the 4TU repository with doi 10.4121/a02c36b4-e689-4181-87d5-cd8ce3b75579.

Received: 2 August 2024; Accepted: 12 November 2024;

Published online: 21 November 2024

References

1. Droppo, I. G. Rethinking what constitutes suspended sediment. *Hydrol. Process.* **15**, 1551–1564 (2001).
2. Dyer, K. R. Sediment processes in estuaries: future research requirements. *J. Geophys. Res.* **94**, 14327–14339 (1989).
3. Winterwerp, J. On the flocculation and settling velocity of estuarine mud. *Cont. Shelf Res.* **22**, 1339–1360 (2002).
4. Mietta, F., Chassagne, C., Manning, A. J. & Winterwerp, J. C. Influence of shear rate, organic matter content, pH and salinity on mud flocculation. *Ocean Dyn.* **59**, 751–763 (2009).
5. Lasareva, E. V. & Parfenova, A. M. Influence of organic matter on the transport of mineral colloids in the river-sea transition zone. in *Oceanography - Relationships of the Oceans With the Continents, Their Biodiversity and the Atmosphere*, 4th edn, Ch. 4 (IntechOpen, London, 2023).
6. Safar, Z. et al. Characterization and classification of estuarine suspended particles based on their inorganic/organic matter composition. *Front. Mar. Sci.* **9**, 896163 (2022).
7. Deng, Z., He, Q., Safar, Z. & Chassagne, C. The role of algae in fine sediment flocculation: In-situ and laboratory measurements. *Mar. Geol.* **413**, 71–84 (2019).
8. van Leussen, W. The variability of settling velocities of suspended fine-grained sediment in the Ems estuary. *J. Sea Res.* **41**, 109–118 (1999).
9. Deng, Z., Huang, D., He, Q. & Chassagne, C. Review of the action of organic matter on mineral sediment flocculation. *Front. Earth Sci.* **10**, 965919 (2022).
10. Gratiot, N. et al. Sediment flocculation in the Mekong River estuary, Vietnam, an important driver of geomorphological changes. *Comptes Rendus Geosci.* **349**, 260–268 (2017).
11. Nicholas, A. & Walling, D. The significance of particle aggregation in the overbank deposition of suspended sediment on river floodplains. *J. Hydrol.* **186**, 275–293 (1996).
12. Bungartz, H. & Wanner, S. C. Significance of particle interaction to the modelling of cohesive sediment transport in rivers. *Hydrol. Process.* **18**, 1685–1702 (2004).
13. Lamb, M. P. et al. Mud in rivers transported as flocculated and suspended bed material. *Nat. Geosci.* **13**, 566–570 (2020).
14. Fettweis, M. Uncertainty of excess density and settling velocity of mud flocs derived from in situ measurements. *Estuar. Coast. Shelf Sci.* **78**, 426–436 (2008).
15. Winterwerp, J. C., van Kessel, T., van Maren, D. S. & van Prooijen, B. *C.Fine Sediment in Open Water. From Fundamentals to Modeling* (Advanced Series on Open Engineering - volume 55. World Scientific., Singapore, 2021). www.worldscientific.com.
16. Torres, M. A. et al. Model predictions of long-lived storage of organic carbon in river deposits. *Earth Surf. Dyn.* **5**, 711–730 (2017).
17. Edmonds, D. A. & Slingerland, R. L. Significant effect of sediment cohesion on delta morphology. *Nat. Geosci.* **3**, 105–109 (2010).
18. He, Q. & Walling, D. E. Spatial variability of the particle size composition of overbank floodplain deposits. *Water, Air, Soil Pollut.* **99**, 71–80 (1997).
19. Aalto, R., Lauer, J. W. & Dietrich, W. E. Spatial and temporal dynamics of sediment accumulation and exchange along Strickland River floodplains (Papua New Guinea) over decadal-to-centennial timescales. *J. Geophys. Res. Earth Surf.* **113** (2008).
20. Ongley, E. D., Krishnappan, B. G., Droppo, G., Rao, S. S. & Maguire, R. J. Cohesive sediment transport: emerging issues for toxic chemical management. *Hydrobiologia* **235-236**, 177–187 (1992).
21. Li, Z., Schieber, J. & Pedersen, P. K. On the origin and significance of composite particles in mudstones: Examples from the Cenomanian Dunvegan Formation. *Sedimentology* **68**, 737–754 (2021).
22. Guo, L. & He, Q. Freshwater flocculation of suspended sediments in the Yangtze River, China. *Ocean Dyn.* **61**, 371–386 (2011).
23. Baas, J. H., Best, J. L. & Peakall, J. Predicting bedforms and primary current stratification in cohesive mixtures of mud and sand. *J. Geol. Soc.* **173**, 12–45 (2016).
24. Wysocki, N. & Hajek, E. Mud in sandy riverbed deposits as a proxy for ancient fine-sediment supply. *Geology* **49.8**, 931–935 (2021).

25. Mooneyham, C. & Strom, K. Deposition of suspended clay to open and sand-filled framework gravel beds in a laboratory flume. *Water Resour. Res.* **54**, 323–344 (2018).
26. Schieber, J., Southard, J. & Thaisen, K. Accretion of mudstone beds from migrating floccule ripples. *Science* **318**, 1760–1763 (2007).
27. Schieber, J. & Southard, J. B. Bedload transport of mud by floccule ripples—Direct observation of ripple migration processes and their implications. *Geology* **37**, 483–486 (2009).
28. Yu, M. et al. Persistent reshaping of cohesive sediment towards stable flocs by turbulence. *Sci. Rep.* **13**, 1760 (2023).
29. Shakeel, A., Safar, Z., Ibanez, M., van Paassen, L. & Chassagne, C. Flocculation of clay suspensions by anionic and cationic polyelectrolytes: a systematic analysis. *Minerals* **10**, 999 (2020).
30. Van Leussen, W. Aggregation of particles, settling velocity of mud flocs a review. *Physical processes in estuaries*. 347–403 (Berlin, Heidelberg: Springer Berlin Heidelberg, 1988).
31. Ye, L., Wu, J., Huang, M. & Yan, J. The role of suspended extracellular polymeric substance (EPS) on equilibrium flocculation of clay minerals in high salinity water. *Water Res.* **244**, 120451 (2023).
32. Ye, L., Penaloza-Giraldo, J. A., Manning, A. J., Holyoke, J. & Hsu, T.-J. Biophysical flocculation reduces variability of cohesive sediment settling velocity. *Commun. Earth Environ.* **4**, 138 (2023).
33. Pérez, K. et al. Estimating the shear resistance of flocculated kaolin aggregates: effect of flocculation time, flocculant dose, and water quality. *Polymers* **14**, 1381 (2022).
34. de Lange, S. I. et al. The impact of flocculation on in situ and ex situ particle size measurements by laser diffraction. *Water Resour. Res.* **60**, e2023WR035176 (2024).
35. Parchure, T. M. & Mehta, A. J. Erosion of soft cohesive sediment deposits. *J. Hydraul. Eng.* **111**, 1308–1326 (1985).
36. Mehta, A. J. & Partheniades, F. An investigation of the depositional properties of flocculated fine sediments. *J. Hydraul. Res.* **13**, 1975 (1975).
37. Chassagne, C. & Safar, Z. Modelling flocculation: towards an integration in large-scale sediment transport models. *Mar. Geol.* **430**, 106361 (2020).
38. Kirca, V. S. O., Saghebian, S. M., Roushangar, K. & Yagci, O. Influence of surface roughness of dune bedforms on flow and turbulence characteristics. *Int. J. Sediment. Res.* **35**, 666–678 (2020).
39. Grangeon, T., Legout, C., Esteves, M., Gratiot, N. & Navratil, O. Variability of the particle size of suspended sediment during highly concentrated flood events in a small mountainous catchment. *J. Soils Sediment.* **12**, 1549–1558 (2012).
40. Allen, J. *Sedimentary Structures: Their Character and Physical Basis*, 1st edn, Vol. 30 (Developments in Sedimentology, Elsevier, Amsterdam, 1982).
41. Kennedy, J. F. The mechanics of dunes and antidunes in erodible-bed channels. *J. Fluid Mech.* **16**, 521–544 (1963).
42. Venditti, J. G. & Bradley, R. W. Bedforms in sand bed rivers. in *Treatise on Geomorphology*, 2nd edn, Vol. 6.1 (eds John (Jack) F. & Schroder), Ch 6.13, 222–254 (Elsevier, Academic Press, 2022).
43. van Rijn, L. Sediment transport, part III: bedforms and alluvial roughness. *J. Hydraul. Eng.* **110**, 1733–1754 (1984).
44. Best, J. The fluid dynamics of river dunes: a review and some future research directions. *J. Geophys. Res. Earth Surf.* **110**, 1–21 (2005).
45. Schindler, R. J. et al. Sticky stuff: Redefining bedform prediction in modern and ancient environments. *Geology* **43**, 399–402 (2015).
46. de Lange, S. et al. Fine sediment in mixed sand-silt environments impacts bedform geometry by altering sediment mobility. *WRF* **60**, e2024WR037065 (2024).
47. Parsons, D. R. et al. The role of biophysical cohesion on subaqueous bed form size. *Geophys. Res. Lett.* **43**, 1566–1573 (2016).
48. Grant, J., Bathmann, U. & Mills, E. The interaction between benthic diatom films and sediment transport. *Estuar. Coast. Shelf Sci.* **23**, 225–238 (1986).
49. Russell, C. E., Fernández, R., Parsons, D. R. & Gabbott, S. E. Plastic pollution in riverbeds fundamentally affects natural sand transport processes. *Commun. Earth Environ.* **4**, 255 (2023).
50. Wan, Z. Bed material movement in hyperconcentrated flow. *J. Hydraul. Eng.* **111**, 987–1002 (1985).
51. Hasan, A. & Fatehi, P. Cationic kraft lignin-acrylamide as a flocculant for clay suspensions: 1. Molecular weight effect. *Sep. Purif. Technol.* **207**, 213–221 (2018).
52. Droppo, I. G. Biofilm structure and bed stability of five contrasting freshwater sediments. *Mar. Freshw. Res.* **60**, 690–699 (2009).
53. Zhang, F., Chen, X., Liu, J. & Zhang, Y. A new countermeasure to deep-sea mining sediment plumes: Using flocculant to enhance particles settling. *Appl. Ocean Res.* **142**, 103811 (2024).
54. Ali, W., Enthoven, D., Kirichek, A., Chassagne, C. & Helmons, R. Effect of flocculation on turbidity currents. *Front. Earth Sci.* **10**, 1014170 (2022).
55. Safar, Z., Deng, Z. & Chassagne, C. Applying a logistic growth equation to model flocculation of sediment in the presence of living and dead organic matter. *Front. Mar. Sci.* **10**, 1227849 (2023).
56. Manning, A. & Dyer, K. A laboratory examination of floc characteristics with regard to turbulent shearing. *Tech. Rep.* www.elsevier.nl/locate/margeo (1999).
57. Kolmogorov, A. Dissipation of energy in locally isotropic turbulence. *C.R. Acad. Sci. URSS.* **32**, 19–21 (1941).
58. Kolmogorov, A. The local structure of turbulence in incompressible viscous fluid for very large Reynolds numbers. *C.R. Acad. Sci. URSS.* **30**, 301 (1941).
59. Bennett, S. J. & Best, J. L. Mean flow and turbulence structure over fixed, two-dimensional dunes: implications for sediment transport and bedform stability. *Sedimentology* **42**, 491–513 (1995).
60. Kwoil, E., Venditti, J. G., Bradley, R. W. & Winter, C. Flow structure and resistance over subaqueous high- and low-angle dunes. *J. Geophys. Res. Earth Surf.* **121**, 545–564 (2016).
61. Lefebvre, A. & Cisneros, J. The influence of dune lee side shape on time-averaged velocities and turbulence. *Earth Surf. Dyn.* **11**, 575–591 (2023).
62. Baas, J. H., Davies, A. G. & Malarkey, J. Bedform development in mixed sand–mud: The contrasting role of cohesive forces in flow and bed. *Geomorphology* **182**, 19–32 (2013).
63. Wu, X., Fernandez, R., Baas, J. H., Malarkey, J. & Parsons, D. R. Discontinuity in equilibrium wave-current ripple size and shape and deep cleaning associated with cohesive sand-clay beds. *J. Geophys. Res. Earth Surf.* **127**, e2022JF006771 (2022).
64. Thomas, R. G. et al. Inclined heterolithic stratification—Terminology, description, interpretation and significance. *Sediment. Geol.* **53**, 123–179 (1987).
65. Nichols, G. J., Cripps, J. A., Collinson, M. E. & Scott, A. C. Experiments in waterlogging and sedimentology of charcoal: results and implications. *Palaeogeogr. Palaeoclimatol. Palaeoecol.* **164**, 43–56 (2000).
66. Baas, J. H. A flume study on the development and equilibrium morphology of current ripples in very fine sand. *Sedimentology* **41**, 185–209 (1994).
67. Baas, J. H. An empirical model for the development and equilibrium morphology of current ripples in fine sand. *Sedimentology* **46**, 123–138 (1999).
68. Soulsby, R. L., Whitehouse, R. J. & Marten, K. V. Prediction of time-evolving sand ripples in shelf seas. *Cont. Shelf Res.* **38**, 47–62 (2012).
69. Allen, J. R. Computational models for dune time-lag: calculations using Stein’s rule for dune height. *Sediment. Geol.* **20**, 165–216 (1978).
70. Yalin, M. Geometrical properties of sand wave. *J. Hydraul. Eng.* **90**, 105–119 (1964).
71. Karim, F. Bed configuration and hydraulic resistance in alluvial-channel flows. *J. Hydraul. Eng.* **121**, 15–25 (1995).

72. Bradley, R. W. & Venditti, J. G. Transport scaling of dune dimensions in shallow flows. *J. Geophys. Res. Earth Surf.* **124**, 526–547 (2019).
73. Malarkey, J. et al. The pervasive role of biological cohesion in bedform development. *Nat. Commun.* **6**, 6257 (2015).
74. Milligan, T. & Loring, D. The effect of flocculation on the size distributions of bottom sediment in coastal inlets: implications for contaminant transport. *Water Air Soil Pollut.* **99**, 33–42 (1997).
75. Crawford, S. E. et al. Remobilization of pollutants during extreme flood events poses severe risks to human and environmental health. *J. Hazard. Mater.* **421**, 126691 (2022).
76. Wölz, J. et al. In search for the ecological and toxicological relevance of sediment re-mobilisation and transport during flood events. *J. Soils Sediment.* **9**, 1–5 (2009).
77. Laursen, S., Fruergaard, M. & Andersen, T. Rapid flocculation and settling of positively buoyant microplastic and fine-grained sediment in natural seawater. *Mar. Pollut. Bull.* **178**, 113619 (2022).
78. Andersen, T. J., Rominikan, S., Olsen, I. S., Skinnebach, K. H. & Fruergaard, M. Flocculation of PVC microplastic and fine-grained cohesive sediment at environmentally realistic concentrations. *Biol. Bull.* **240**, 42–51 (2021).
79. Yan, M., Wang, L., Dai, Y., Sun, H. & Liu, C. Behavior of Microplastics in Inland Waters: Aggregation, Settlement, and Transport. *Bull. Environ. Contam. Toxicol.* **107**, 700–709 (2021).
80. Geyer, R., Jambeck, J. R. & Law, K. L. Production, use, and fate of all plastics ever made. *Sci. Adv.* **3**, e1700782 (2017).
81. Martinius, A. & van den Berg, J. *Atlas of sedimentary structures in estuarine and tidally-influenced river deposits of the Holocene Rhine-Meuse-Scheldt system: Their application to the interpretation of analogous outcrop and subsurface depositional systems* (EAGE Publications bv, 2011).
82. Dalrymple, R. W. & Choi, K. Morphologic and facies trends through the fluvial–marine transition in tide-dominated depositional systems: a schematic framework for environmental and sequence-stratigraphic interpretation. *Earth Sci. Rev.* **81**, 135–174 (2007).
83. Potter, P. E., Maynard, J. B. & Pryor, W. A. *Sedimentology of Shale* (Springer New York, New York, NY, 1980).
84. Potter, P. E., Maynard, J. B. & Depetris, P. J. *Mud and Mudstones: Introduction and Overview* (Springer Science & Business Media, 2005).
85. van Kessel, T., Vanlede, J. & de Kok, J. Development of a mud transport model for the Scheldt estuary. *Cont. Shelf Res.* **31**, S165–S181 (2011).
86. van Rijn, L. C. & Grasmeijer, B. Effect of channel deepening on tidal flow and sediment transport—part II: muddy channels. *Ocean Dyn.* **68**, 1481–1501 (2018).
87. Verney, R., Lafite, R., Claude Brun-Cottan, J. & Le Hir, P. Behaviour of a floc population during a tidal cycle: Laboratory experiments and numerical modelling. *Cont. Shelf Res.* **31**, S64–S83 (2011).
88. Fugate, D. C. & Friedrichs, C. T. Controls on suspended aggregate size in partially mixed estuaries. *Estuar. Coast. Shelf Sci.* **58**, 389–404 (2003).
89. Becker, M. et al. Formation and entrainment of fluid mud layers in troughs of subtidal dunes in an estuarine turbidity zone. *J. Geophys. Res. Oceans* **118**, 2175–2187 (2013).
90. van Ledden, M., van Kesteren, W. & Winterwerp, J. A conceptual framework for the erosion behaviour of sand–mud mixtures. *Cont. Shelf Res.* **24**, 1–11 (2004).
91. Avnimelech, Y., Troeger, B. W. & Reed, L. W. Mutual flocculation of algae and clay: evidence and implications. *Science* **216**, 63–65 (1982).
92. Stross, R. & Sokol, R. Runoff and flocculation modify underwater light environment of the Hudson River Estuary. *Estuar. Coast. Shelf Sci.* **29**, 305–316 (1989).
93. Lu, C. et al. The influences of a clay lens on the hyporheic exchange in a sand dune. *Water* **10**, 826 (2018).
94. Pillai, J. Flocculants and coagulants: the keys to water and waste management in aggregate production. Nalco Company. Reprint R-680. *Tech. Rep.* [https://aniq.org.mx/pqta/pdf/Respaldo/Flocculants%20and%20Coagulants%20NALCO%20\(LIT\).pdf](https://aniq.org.mx/pqta/pdf/Respaldo/Flocculants%20and%20Coagulants%20NALCO%20(LIT).pdf) (1997).
95. BASF. Zetag® 8125 Solid grade cationic polyelectrolyte. *Tech. Rep.* https://download.basf.com/p1/000000000030845598_SDS_GEN_00/en_UN/Zetag_8125-AP_30845598_SDS_GEN_00_en_1-0.pdf (2013).
96. Romero, C. P., Jeldres, R. I., Quezada, G. R., Concha, F. & Toledo, P. G. Zeta potential and viscosity of colloidal silica suspensions: effect of seawater salts, pH, flocculant, and shear rate. *Colloids Surf. A Physicochem. Eng. Asp.* **538**, 210–218 (2018).
97. Whitehouse, R., Soulsby, R., Roberts, W. & Mitchener, H. *Dynamics of estuarine muds* (Thomas Telford Publishing, 2000).
98. Wan, Z. & Wang, Z. *Hyperconcentrated Flow* (Taylor and Francis, New York, 1994).
99. van den Berg, J. & van Gelder, A. A new bedform stability diagram, with emphasis on the transition of ripples to plane bed in flows over fine sand and silt. *Spec. Publ. Int. Ass. Sediment.* **17**, 11–21 (1993).
100. Krishnappan, B. G. Cohesive sediment transport studies using a rotating circular flume. In *Proc. 7th International Conference on Hydroscience and Engineering* <https://www.researchgate.net/publication/294260969> (2006).
101. Gibbs, R. J. Floc breakage by pumps. *J. Sediment. Res.* **51**, 670–672 (1981).
102. Partheniades, E., Cross, R. H. & Ayora, A. Further results on the deposition of cohesive sediments. *Coast. Eng.* 1968. 723–742 <https://doi.org/10.1061/9780872620131.0> (1968).
103. Baar, A. W., Weisscher, S. A. & Kleinhans, M. G. Interaction between lateral sorting in river bends and vertical sorting in dunes. *Sedimentology* **67**, 606–626 (2020).
104. Petersen, O. & Krishnappan, B. G. Measurement and analysis of flow characteristics in a rotating circular flume. *J. Hydraul. Res.* **32**, 483–494 (1994).
105. Spork, V. *Erosionsverhalten feiner Sedimente und ihre biogene Stabilisierung*. Ph.D. thesis, Wasserbau und Wasserwirtschaft, Aachen (1997).
106. Ye, L., Manning, A. J. & Hsu, T.-J. Oil-mineral flocculation and settling velocity in saline water. *Water Res.* **173**, 115569 (2020).
107. MacIver, M. Safas: sedimentation and floc analysis software (2019).
108. Vermeulen, B. Adcptools: set of functions to process acoustic Doppler current profiler data (2015).
109. Van der Mark, C. F. & Blom, A. A new and widely applicable tool for determining the geometric properties of bedforms, CE&M Research Report 2007R-003/WEM-002 ISSN 1568-4652, University of Twente, Enschede, Netherlands (2007).

Acknowledgements

SdL and TH were funded by the Netherlands Organisation for Scientific Research (NWO), within Vici project “Deltas out of shape: regime changes of sediment dynamics in tide-influenced deltas” (Grant NWO-TTW 17062). KW was funded by the Sectorplan Techniek for strengthening the Technical Sciences at Wageningen University. Part of this work was conducted as the MSc thesis by AvdW. The authors would like to thank Deltares for using their experimental facilities in the framework of the MoU between TU Delft/Deltares, and Professor Schüttrumpf for providing access and resources of the experimental facilities of IWW at RWTH Aachen University. Thanks to Bart Vermeulen for his help with scripting, and David Boelee and the laboratory technicians at RWTH Aachen University for their help with the technical setup.

Author contributions

S.d.L.: conceptualisation, data collection, data analysis, data interpretation, manuscript drafting, visualisation, revision of manuscript. A.v.d.W.: data

collection, data analysis, data interpretation. C.C.: data collection, revision of manuscript. W.A.: data collection, revision of manuscript. A.H.: data interpretation, revision of manuscript, supervision. M.B.: data collection, revision of manuscript. K.B.: data collection. K.W.: conceptualisation, data collection, revision of manuscript, supervision.

Competing interests

The authors declare no competing interests.

Additional information

Supplementary information The online version contains supplementary material available at <https://doi.org/10.1038/s43247-024-01901-x>.

Correspondence and requests for materials should be addressed to Sjoukje I. de Lange.

Peer review information *Communications Earth & Environment* thanks Enrica Viparelli and the other, anonymous, reviewer(s) for their contribution to the peer review of this work. Primary Handling Editor: Alireza Bahadori. A peer review file is available.

Reprints and permissions information is available at <http://www.nature.com/reprints>

Publisher's note Springer Nature remains neutral with regard to jurisdictional claims in published maps and institutional affiliations.

Open Access This article is licensed under a Creative Commons Attribution 4.0 International License, which permits use, sharing, adaptation, distribution and reproduction in any medium or format, as long as you give appropriate credit to the original author(s) and the source, provide a link to the Creative Commons licence, and indicate if changes were made. The images or other third party material in this article are included in the article's Creative Commons licence, unless indicated otherwise in a credit line to the material. If material is not included in the article's Creative Commons licence and your intended use is not permitted by statutory regulation or exceeds the permitted use, you will need to obtain permission directly from the copyright holder. To view a copy of this licence, visit <http://creativecommons.org/licenses/by/4.0/>.

© The Author(s) 2024